



Rapid injection molding of high-aspect-ratio nanostructures

Shuntaro Hattori, Keisuke Nagato *, Tetsuya Hamaguchi, Masayuki Nakao

Department of Mechanical Engineering, Graduate School of Engineering, The University of Tokyo, 7-3-1 Hongo, Bunkyo-ku, Tokyo 113-8656, Japan

ARTICLE INFO

Article history:

Received 13 September 2009

Received in revised form 4 November 2009

Accepted 8 November 2009

Available online 12 November 2009

Keywords:

Injection molding

High-aspect-ratio nanostructures

Dynamic heating

ABSTRACT

The authors have developed a method for thermal injection molding of high-aspect-ratio nanostructures involving dynamic heating of the mold surface. The conventional injection molding of nanostructures is difficult to achieve because of the rapid formation of a solidified layer caused by high thermal flux from the melted polymer to the cold mold. In our system, a nanostructured mold surface was heated during polymer filling and then immediately cooled by the mold bases, which are kept at a lower temperature. Using polystyrene, we demonstrated the replication of line-and-space (pitch: 800 nm, depth: 400 nm) and cone patterns (pitch: 200 nm, depth: 400 nm) with a cycle time of less than 15 s.

© 2009 Elsevier B.V. All rights reserved.

1. Introduction

Nanostructured surfaces are known to have various potential applications including optical devices, optical memories, and bioanalysis templates. For the mass production of these nanostructures, methods of nanoimprint lithography and nanomolding are being intensively researched and developed, in which a thin film on a substrate or bulk material surface is formed by pressing a nanostructured mold [1–5]. Recently, high-aspect-ratio nanostructures (HARNs) have attracted much attention owing to their applications such as antireflection structures [6] and bioanalysis sheets [7].

Here, thermal injection molding is intrinsically advantageous in terms of its high throughput. In injection molding, a preheated and melted polymer is injected into a mold cavity. The molds are kept under the glass transition temperature (T_g) of the polymer so that the polymer can be rapidly solidified and demolded. Therefore, injection molding has a short cycle time. Injection molding also has an advantage in terms of the flexibility of component shape. Thus, injection molding is used to produce wide range of products at low cost. However, the replication of HARNs using injection molding is difficult because the surface of the injected polymer is solidified as soon as the polymer touches the mold and it is thus difficult to fill the cavities of nanostructures [8–11]. On the other hand, the concept of local heating of the mold surface has been applied to nanomolding and nanoimprint lithography for high-throughput replication. Local heating by light [12] or Joule heating [13] requires low energy and has a high cooling rate.

In this study, we propose and develop a new injection molding system involving dynamic heating of the mold surface for the rapid replication of HARNs. The mold surface is locally heated to above T_g only during the filling of the nanostructures, then the polymer replica and mold surface are cooled by the mold base, which is kept below T_g . This method enables the rapid replication of HARNs.

2. Injection molding with dynamic heating of mold surface

When the temperature of the mold surface is above T_g , the injected polymer is not solidified and is easily filled in the nanostructure cavity. Therefore, the main functional requirement of the system is that the mold surface is kept above T_g during the polymer filling.

Fig. 1 shows a schematic of our injection molding method involving the dynamic heating of the mold surface. A thin-film heater set under the nanostructured stamper heats the stamper surface. More powerful heating in a shorter time prevents heat from diffusing to the mold base, thus the cooling time is shorter. Immediately after the nanostructure cavity is filled with the polymer, the thin-film heater is turned off and the heat provided by the injected polymer and thin-film heater is rapidly removed by the mold base, which is kept below T_g . In this system, components with HARNs can be produced with as high throughput as conventional injection molding.

3. Experimental

The designed dynamic heating injection molding system and experimental details are described as follows. We fabricated the thin-film heater by sputtering Cr as a conducting layer (thickness: 500 nm) and SiO_2 as an insulating layer (thickness: 1 μm) on a

* Corresponding author.

E-mail address: nagato@hnl.t.u-tokyo.ac.jp (K. Nagato).

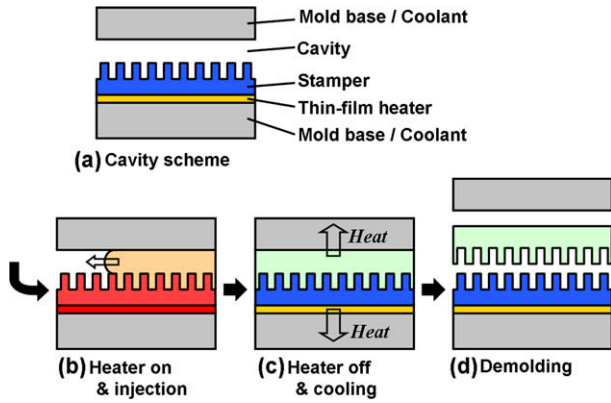


Fig. 1. (Color online) Schematic of injection nanomolding with dynamic heating of mold surface.

polished AlN substrate (thickness: 2 mm, thermal conductivity: 160 W/m K). This heater was additionally covered with a polyimide sheet tape (thickness: 75 μm) for better insulation. This thin-film heater and a 300- μm -thick electroplated Ni stamper are fixed on a mold base (A7075, JIS, thermal conductivity: 130 W/m K) by screws together with a frame washer of 2 mm thickness and an inner size of $33 \times 38 \text{ mm}^2$. The opposite mold base (A7075) is polished and a sprue bush is set at its center. The replica part corresponding to the sprue bush is called a sprue and its shape is a truncated cone with dimensions of $\phi 2/\phi 4 \times 35 \text{ mm}$. Therefore, the nanostructured surface of the replica directly faces the sprue. A thermocouple is made by welding a 25- μm -diameter chromel wire and an alumel wire and is sandwiched between the heater and the Ni stamper to measure the temperature of the Ni stamper. Another thermocouple (6193B, Kistler) placed on the mold base at the side of the sprue is used to monitor the temperature of the mold surface opposite the stamper. A pressure sensor (6183AE, Kistler) is also set at the cavity surface opposite the stamper. We used polystyrene (PS, T_g : 105 $^\circ\text{C}$, molecular weight: 100,000) as the material for injection molding with a Roboshot S-2000i5A (Fanuc, Ltd.) injection molding machine. Liquid-phase PS heated to 240 $^\circ\text{C}$ is injected from the nozzle immediately after the thin-film heater reaches its target temperature, and then the heater is turned off. The injected replica is cooled by both mold bases.

We used two different Ni stampers with a line-and-space pattern and a conical-hole pattern. Fig. 2a shows cross-section images of the line-and-space pattern obtained using a scanning electron

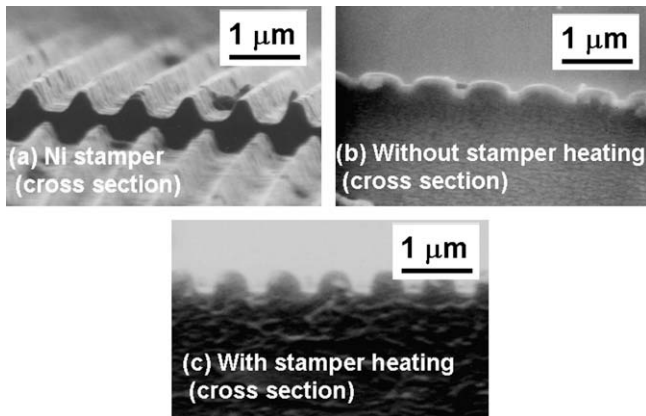


Fig. 2. SEM images of Ni mold (a) and molded PS surfaces directly below the sprue obtained by injection molding without (b) and with stamper heating (c) (800-nm-pitch line-and-space pattern).

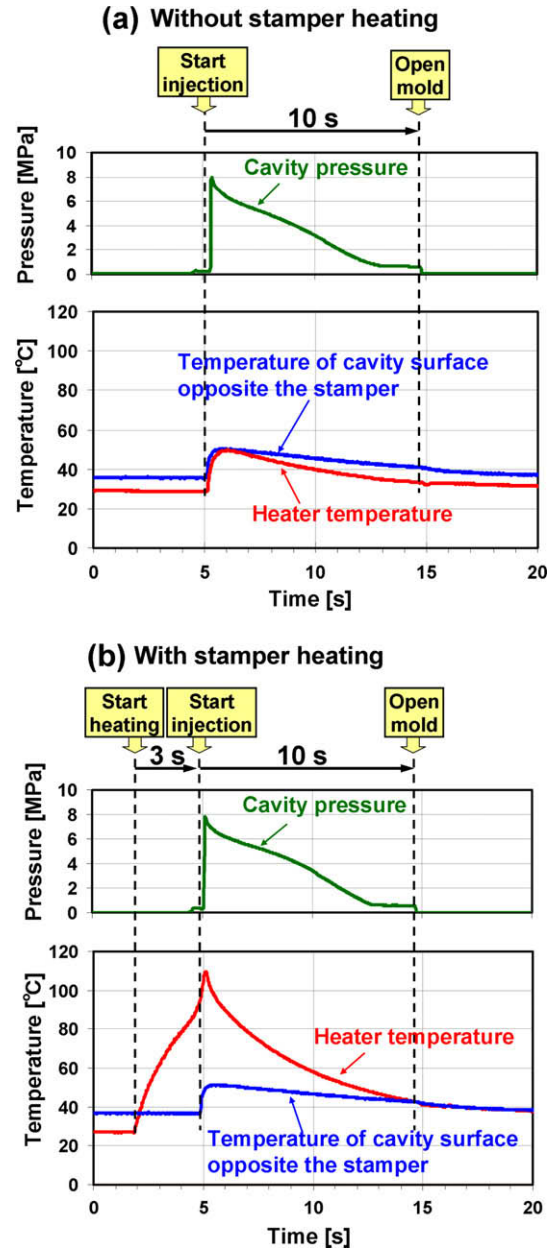


Fig. 3. (Color online) Typical time profiles of temperatures of heater surface and cavity surface opposite the stamper and the cavity pressure used for injection molding without (a) and with stamper heating (b).

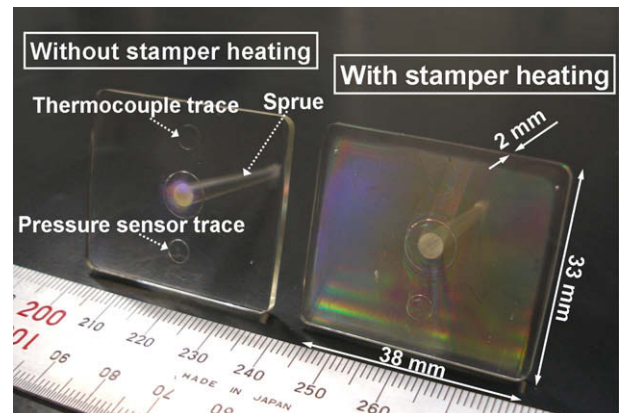


Fig. 4. (Color online) Photographs of replicas obtained by injection molding without and with stamper heating (800-nm-pitch line-and-space pattern).

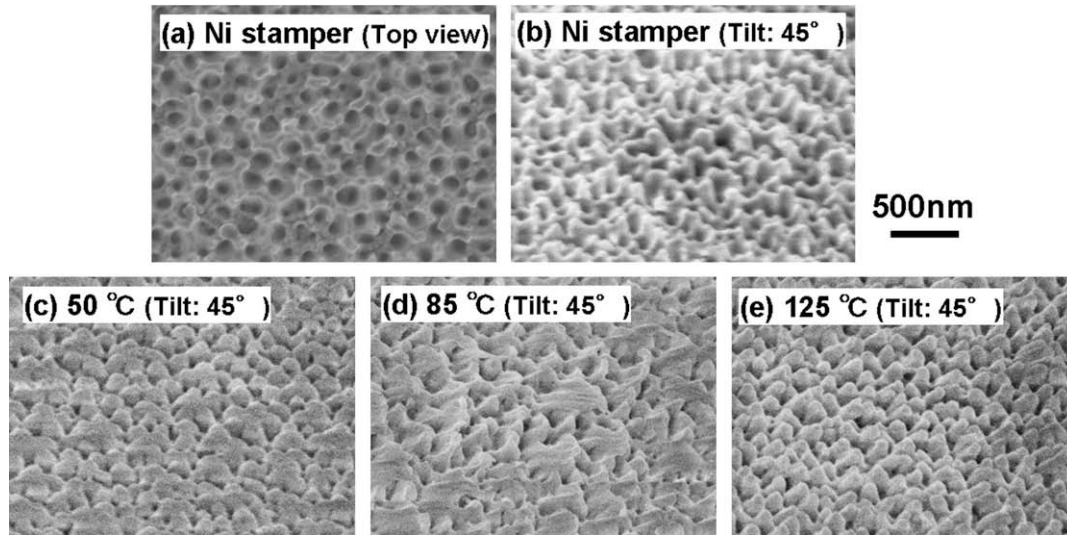


Fig. 5. SEM images of Ni mold (a, b) and molded PS surfaces directly below the sprue obtained by injection molding with heater temperatures during injection of 50 °C (c), 85 °C (d), and 125 °C (e).

microscope (SEM, S-4160: Hitachi). The pitch and depth of the pattern are 800 and 400 nm, respectively. We compare the results without and with stamper heating. The peak temperature of the thin-film heater was set to about 110 °C. The random conical-hole pattern (Fig. 5a and b) [14] has an average pitch and depth of 200 and 400 nm, respectively; thus, the aspect ratio of the holes is approximately 2. This pattern was fabricated to replicate an antireflection surface. Using the stamper with this pattern, we verified the moldability when peak temperature of the stamper were 50, 85 and 125 °C.

4. Results and discussion

Fig. 3a and b shows typical time profiles of the temperatures of the heater and cavity surface and the cavity pressure without and with stamper heating, respectively. The mold base on the side of the sprue bush was heated to 38 °C by the injection nozzle while the mold base on the stamper side was reduced to 24 °C (room temperature). The peak cavity pressure was 8 MPa, which then linearly decreased to 0.8 MPa in 8 s. This pressure reduction is caused by the reduction in thermal volume of the replica, i.e., shrinkage occurred. However, because the pressure did not reach 0, the shrinkage did not cause replication lack. The replication results will be described after. The times from the closing the mold and the following injection to opening the mold were 10 and 13 s in the experiments without and with stamper heating, respectively. The difference of 3 s corresponds to the time required for heating the stamper to the target temperature. The cooling time was almost the same in both cases. Since the cooling rate depends on the thermal conductivities of the heater substrate and mold base, the cooling time, which depends on the cycle time, is approximately proportional to the thickness of the replica.

Fig. 2 shows SEM images of the Ni stamper (a) and the replica surface fabricated without (b) and with (c) stamper heating (heater temperature: 110 °C). The pitch and depth of the Ni stamper are 800 and 400 nm, respectively. The surface molded without stamper heating has 150-nm-high ridges; on the other hand, that molded with stamper heating has 400-nm-deep trenches. Comparing the surfaces far from the sprue (more than 10 mm), the height of the ridges obtained without stamper heating was less than 50 nm, whereas the structure obtained with stamper heating was almost the same as that in Fig. 2c. Fig. 4 shows photographs of

the replicas obtained by the two processes. The replica molded without stamper heating has a low diffraction intensity only near the sprue (Fig. 4a). The unevenness of the moldability is occurred because the stamper surface at the region directly under the sprue was heated more than elsewhere. On the other hand, the replica molded with stamper heating has a high diffraction intensity over the whole surface (Fig. 4b). Two circular traces (ϕ 4 mm) can be observed on the backside of the nanostructured surface due to the thermocouple and pressure sensor.

We also demonstrated replication using a stamper with a conical-hole array pattern (Fig. 5a and b). The peak temperatures during injection were set at 50, 85, and 125 °C. Fig. 5c–e shows SEM images (tilt angle: 45°) of replica surfaces obtained with each heater temperature. The images show the surfaces obtained directly below the sprue. The moldability of the surface was greatest for the highest heater temperature. The replica obtained with the heater temperature of 125 °C shown in Fig. 5e exhibited similar nanostructures over the whole area. However, those obtained at 50 and 85 °C had poorer moldability further from the center (directly opposite the sprue). These results indicate that maintaining the mold surface above T_g results in better moldability.

5. Conclusions

We have proposed and demonstrated a new advanced nano-molding process based on injection molding. To avoid the formation of a solidified layer on the contact surface of the polymer, we heated the mold surface using a thin-film heater at the back of a Ni stamper while filling the cavity with polymer. Using this system, 800- and 200-nm-pitch nanostructures with an aspect ratio of 1–2 were replicated, and the effectiveness of mold surface heating was demonstrated. Injection molding with dynamic heating of the mold surface is expected to not only lead to the high-throughput production of replicas with a nanostructured surface but also enable the fabrication of device applications with complicated shapes such as nonflat optical devices and bioanalysis dishes.

Acknowledgments

The master substrate for the electroplated Ni mold was fabricated using the EB writer (F5112+VD01) at the University of Tokyo VDSI Design and Education Center (VDEC), which was do-

nated by Advantest Corporation. This work was partially supported by Grant-in-Aid for Scientific Research (Nos. 19106003, 21860015) and by the Global Center of Excellence (G-COE) Program “Global Center of Excellence for Mechanical Systems Innovation (GMSI)” from the Ministry of Education, Culture, Sports, Science and Technology, Japan.

References

- [1] L.J. Guo, *J. Phys. D* 37 (2004) R123.
- [2] S.Y. Chou, P.R. Krauss, P.J. Renstrom, *Appl. Phys. Lett.* 67 (1995) 3114.
- [3] H. Schiff, *J. Vac. Sci. Technol. B* 26 (2008) 458.
- [4] H. Schiff, C. David, M. Gabrecht, L.J. Heyderman, W. Kaiser, S. Koppel, L. Scandella, *Microelectron. Eng.* 53 (2000) 171.
- [5] Y.C. Su, J. Shah, L. Lin, *J. Micromech. Microeng.* 14 (2004) 415.
- [6] C.J. Ting, N.C. Huang, H.Y. Tsai, C.P. Chou, C.C. Fu, *Nanotechnology* 19 (2008) 205301.
- [7] K. Kuwabara, M. Ogino, T. Ando, A. Miyauchi, *Appl. Phys. Lett.* 93 (2008) 033904.
- [8] T. Ohta, K. Inoue, T. Ishida, Y. Gotoh, I. Satoh, *Jpn. J. Appl. Phys.* 32 (1993) 5214.
- [9] T. Imai, N. Shida, T. Higuchi, K. Suga, T. Iida, F. Yokogawa, *Jpn. J. Appl. Phys.* 40 (2001) 1661.
- [10] M. Nakao, K. Tsuchiya, T. Sadamitsu, Y. Ichikohara, T. Ohba, T. Ooi, *Int. J. Adv. Manufact. Technol.* 38 (2008) 426.
- [11] Y.E. Yoo, T.H. Kim, D.S. Choi, S.M. Hyun, H.J. Lee, K.H. Lee, S.K. Kim, B.H. Kim, Y.H. Seo, H.G. Lee, J.S. Lee, *Curr. Appl. Phys.* 9 (2009) e12.
- [12] P.-C. Chang, S.-J. Hwang, *J. Appl. Polym. Sci.* 102 (2006) 3704.
- [13] M. Tormen, R. Malureau, R.H. Pedersen, L. Lorenzen, K.H. Rasmussen, C.J. Luscher, A. Kristensen, O. Hansen, *Microelectron. Eng.* 85 (2008) 1229.
- [14] The fabrication method of the stamper is unpublished.